Experimental study of a system for hydrogen permeation from gas phase to liquid sodium

Pietro Brazzale, Aurélien Chassery, Thierry Gilardi, Christian Latgé, Xuân-Mi Meyer, Xavier Joulia

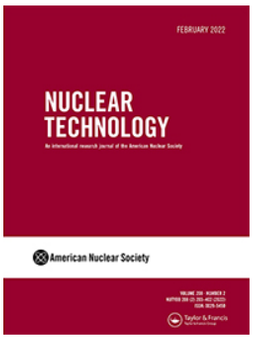

Nuclear Technology

ISSN: (Print) (Online) Journal homepage: www.tandfonline.com/journals/unct20

Experimental Study of a System for Hydrogen Permeation from Gas Phase to Liquid Sodium

Pietro Brazzale, Aurélien Chassery, Thierry Gilardi, Christian Latgé, Xuân-Mi Meyer & Xavier Joulia

To cite this article: Pietro Brazzale, Aurélien Chassery, Thierry Gilardi, Christian Latgé, Xuân-Mi Meyer & Xavier Joulia (2022) Experimental Study of a System for Hydrogen Permeation from Gas Phase to Liquid Sodium, Nuclear Technology, 208:2, 284-294, DOI: 10.1080/00295450.2021.1895661

To link to this article: https://doi.org/10.1080/00295450.2021.1895661

Published online: 12 Jun 2021.

NUCLEAR TECHNOLOGY · VOLUME 208 · 284–294 · FEBRUARY 2022

DOI: https://doi.org/10.1080/00295450.2021.1895661

Experimental Study of a System for Hydrogen Permeation from Gas Phase to Liquid Sodium

Pietro Brazzale,[a]* Aurélien Chassery,[a] Thierry Gilardi,[a] Christian Latgé,[a] Xuân-Mi Meyer,[b] and Xavier Joulia[b]

[a]*CEA, DEN, Cadarache, DTN, F-13108 Saint-Paul-lez-Durance, France*
[b]*Université de Toulouse, Laboratoire de Génie Chimique, CNRS, INPT, UPS, Toulouse, France*

Received December 8, 2020
Accepted for Publication February 23, 2021

Abstract — *In the framework of sodium fast reactors, the management of tritium contamination in the sodium secondary circuit and the control of its release into the atmosphere is fundamental. In order to capture and recover tritium by coprecipitation worth hydrogen in cold traps, it is necessary to maintain a certain amount of hydrogen dissolved in the liquid sodium stream. Hydrogen injection by permeation through nickel membranes has been proposed to provide a continuous hydrogen intake to a liquid sodium stream, allowing the desired hydrogen concentration to be reached. A permeator prototype and the related process have been designed. Permeation tests have been carried out in an experimental facility set up at CEA Cadarache at sodium temperatures from 375°C to 450°C and hydrogen partial pressures from* 5×10^3 *to* 3×10^4 *Pa in order to quantify their influence on hydrogen permeation flux. Measurements on both the gas and sodium sides provide a complete hydrogen content observability over the system. Experimental results show a good agreement with the theoretical permeation laws for hydrogen pressures below* 2×10^4 *Pa and provide an estimation of the temperature dependency of the permeability coefficient, which will be useful for the industrial scale-up of the process.*

Keywords — *Hydrogen, sodium fast reactors, permeation, nickel membrane, tritium.*

Note — *Some figures may be in color only in the electronic version.*

I. INTRODUCTION

For sodium fast reactor (SFR) safety, the management of tritium contamination in coolant circuits to control tritium release to the external environment is a major issue. This can be done by facilitating hydrogen and tritium trapping via cocrystallization as NaH or NaT in purification devices called cold traps[1]; this process requires a certain hydrogen concentration in liquid sodium. During the operation of classical SFRs equipped with an energy conversion system based on a Rankine cycle (with water/steam tertiary circuit), a hydrogen "supply" is provided continuously due to aqueous corrosion inside the steam generator tubes. If this contribution is not sufficient, or in the case of innovative reactors based on a Brayton cycle energy conversion system[2] where aqueous corrosion does not take place, an external and independent device is necessary to introduce continuously the required hydrogen flux into liquid sodium.

The hydrogen mass transfer by permeation through nickel-dense membranes has been identified as a suitable technical solution. A permeator prototype has been designed at CEA to transfer hydrogen from a gas phase to liquid sodium in the temperature range from 350°C to 450°C, corresponding to the operating temperatures of an SFR's secondary circuit. It is composed of four high-purity Ni201 tubes [outer diameter (OD) 7.2 mm, thickness 0.3 mm, length 500 mm], inserted in a stainless steel shell (OD 42 mm).

A previous study[3] has demonstrated that, for enough thick membranes (above 50 μm) and for turbulent sodium

*E-mail: pietrobrazzale@gmail.com

flow rates, the steady-state hydrogen molar permeation rate across a dense membrane in a gas-sodium configuration follows a diffusion-limited process according to Richardson's law[4]:

$$Q_{H2} = \frac{A}{\delta} pe_0 exp^{\frac{-E_p}{RT}} \left(\sqrt{P_{H2,f}} - \sqrt{P_{H2,p}}\right) \quad \left[\text{mol s}^{-1}\right] , \tag{1}$$

where

A = membrane surface (m^2)

δ = membrane thickness (m)

$pe_0 exp^{\frac{-E_p}{RT}}$ = expression to calculate the membrane permeability coefficient (mol m^{-1} s^{-1} $Pa^{-0.5}$)

$P_{H2,f}$, $P_{H2,p}$ = hydrogen partial pressures in feed and permeate sides, respectively, which are constant and homogeneous along the membrane.

When hydrogen is dissolved in a liquid sodium phase, its partial pressure can be expressed by means of Sieverts' equilibrium law. In fact, below the saturation concentration $C^S_{H,Na}(T)$ at a given temperature T, hydrogen is dissolved in liquid sodium in the ionic form H^- (Refs. 5 and 6); previous studies have given measurements of the Sieverts equilibrium constant $K_{S,Na}$ (Ref. 7), which links hydrogen mass concentration $y_{H,Na}$ to its equilibrium partial pressure, as follows:

$$K_{S,Na} = \frac{y_{H,Na}}{\sqrt{P_{H_2}}} \left[\text{ppb Pa}^{-0.5}\right] . \tag{2}$$

Equation (1) combined with Eq. (2) can be used in two opposite transfer ways, when hydrogen is introduced in sodium and when it is extracted; the second case is common in SFRs to obtain measurements of hydrogen concentrations in sodium, in the so called hydrogen meters[8] as for the one used for this study and already tested on the Phenix reactor.[9] However, very few studies were carried out when permeation takes place in the opposite way, from a gas phase to liquid sodium. This work focuses on this case. An experimental campaign has been performed to obtain measurements of hydrogen permeation fluxes through a multitube nickel membrane from a diluted gas phase to liquid sodium and to compare results with the previously discussed theoretical laws.

II. EXPERIMENTAL SETUP AND PROCEDURE

II.A. Experimental Sodium Loop

Tests were carried out in an experimental sodium facility at CEA Cadarache; a detailed flowchart of the circuit is provided in Fig. A.1 in the Appendix. It consists of a main closed loop where liquid sodium can circulate. Moreover, three auxiliary sections, disposed in parallel, can be isolated or connected to the main circuit by opening or closing, respectively, some manual valves, as reported in Fig. 1:

1. The test section (TS), where the permeator prototype and the hydrogen meter (DH) are installed.
2. The plugging meter (PI) section, where a nonspecific measurement of sodium purity is provided.
3. The cold trap (CT) section, where sodium is purified, by flowing though the cold trap.

The main loop is equipped with an electromagnetic pump, which provides a maximum volumetric flowrate of

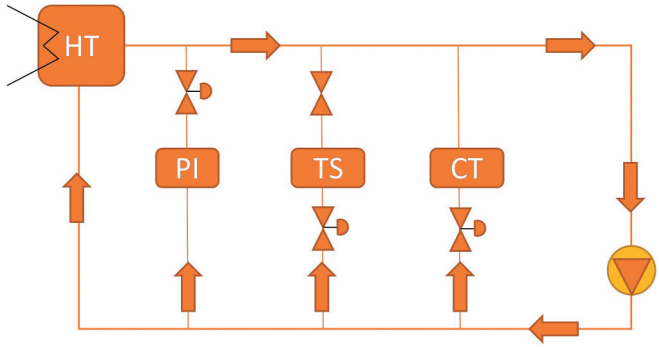

Fig. 1. Experimental sodium loop main components.

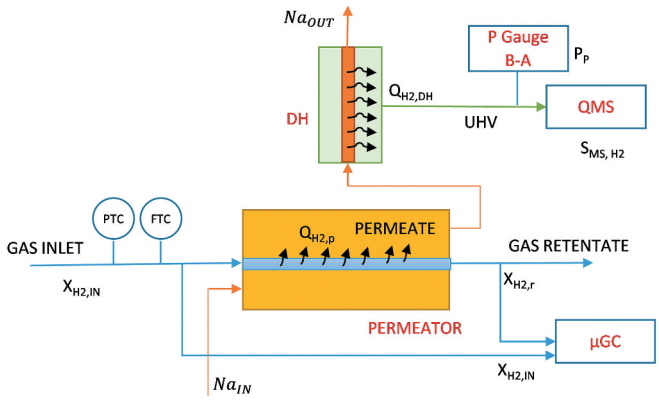

Fig. 2. Test section scheme and measurement devices.

2.5 m^3/h; it can be modified by regulating the pump voltage. A heating tank (HT) is installed on the main circuit, where sodium is heated up by means of electrical resistance heaters. The distribution of the total flow rate into the auxiliary sections can be regulated manually by throttling the valves.

II.B. Test Section

The TS in Fig. A.2 in the Appendix is composed of the permeator prototype, which allows hydrogen introduction into sodium, and the hydrogen meter (DH), which provides a measurement of the hydrogen concentration in sodium; both devices are based on the affinity for hydrogen permeation through nickel membranes. In the first case, a 3% molar H_2/Ar gas mixture circulates inside nickel tubes; the choice of such a diluted feed mixture is imposed by safety rules in the nuclear installations to limit the hydrogen flammability hazard (hydrogen flammability lower limit in air is 4% molar). A part of hydrogen is transferred by permeation, diffusing through nickel's walls to liquid sodium, which continuously flows outside the membranes. This happens thanks to the positive difference of hydrogen partial pressure (i.e., concentration) between the gas and sodium phase, which is obtained during the test conditions described in Sec. III.C. In the hydrogen meter, the reverse process takes place: Liquid sodium containing hydrogen flows inside nickel tubes, while the outer shell is maintained under high-vacuum (HV) conditions in order to reach a very low hydrogen pressure, practically negligible if compared to the sodium side. Thanks to the partial pressure difference, hydrogen diffuses from sodium to the vacuum side, and measuring its equilibrium pressure by mass spectrometry, an estimation of hydrogen concentration in sodium can be obtained. The permeator and hydrogen meter (DH) are installed in series, so that sodium flows before through the permeator, then through the hydrogen meter.

II.C. Gas Supply System

In order to minimize the hydrogen explosion risk, a gas mixture of argon 97%–hydrogen 3% molar concentration is used to feed the permeator. However, this choice does not allow for the use of static gas in the feed side since hydrogen consumption by permeation would reduce progressively its concentration, and consequently the permeation rate, thus providing a nonstationary condition that would be hardly measurable. Therefore, a continuous gas flow is needed inside the permeator in order to maintain controlled conditions and a stable permeation rate through the membranes. To do this, a gas supply system is connected to the permeator inlet and outlet gas sides; a continuous gas flow rate is provided by a bottle containing Ar/H_2 3% (crystal mixture by Air Liquide); the gas pressure P_{gas} can be modified in the range of 1×10^5 to 10×10^5 Pa by a pneumatic valve controlled by a pressure sensor (PTC). The inlet gas flow rate $(Q_{gas\ in})$ can be regulated from 100 to 1000 Nml/min thanks to a mass flowmeter (FTC). Two sampling lines are installed at the permeator inlet and outlet, respectively, connected to a gas chromatograph (μGC) that provides a measurement of the hydrogen molar concentrations into the inlet $(X_{H2\ in})$ and retentate $(X_{H2\ r})$ gas. Pneumatic automated valves and a control system allow remote operations during tests.

II.D. High-Vacuum System

A vacuum system is connected to the hydrogen meter shell in order to enhance hydrogen permeation from the sodium to the vacuum side. The aim is to provide as well a measurement of the permeated hydrogen by means of a so-called residual gas analysis[10] (RGA). It consists of

1. a pumping system composed of a turbo-molecular pump (Agilent) and an ionic pump (Agilent) that allows the system to reach HV conditions around 10^{-8} mbar
2. a Bayard-Alpert Pirani pressure gauge (Inficon, model BPG400)
3. a quadrupole mass spectrometer (QMS), Hiden model HAL201 RC, that provides measurement of permeated hydrogen partial pressure
4. a hydrogen bottle equipped with a calibrated leak, providing a known hydrogen flow rate in order to calibrate the pressure gauge and QMS signals
5. a vacuum piping CF63, connecting the RGA system to the hydrogen meter shell.

The entire HV piping is thermally insulated and electrically traced to be warmed up to a maximum temperature of 200°C; in this way, by regulating the system at a stable value, the temperature influence on pressure and QMS measurement is minimized. Furthermore, moisture and other gases trapped in the metal during standby periods can be easily degassed before starting the permeation test.

III. MEASUREMENT TECNIQUES

To determine the hydrogen molar transfer rate from gas to sodium phase during a permeation test $Q_{H2\ p}$, two

measurement techniques are provided in the gas and sodium phases, respectively. The first one is based on the hydrogen mass balance on the permeator prototype, while the second is provided by hydrogen meter measurements.

III.A. Gas Measurements

By considering the inside of the permeator nickel tubes as a fixed volume, with one inlet (gas feed), one outlet (gas retentate), and one permeate side (liquid sodium), the total [Eq. (3)] and hydrogen [Eq. (4)] mass balances can be applied as follows:

$$Q_{gas\ in} = Q_{gas\ r} + Q_{H2\ p} \quad \left[\text{mol s}^{-1}\right] \tag{3}$$

and

$$Q_{gas\ in}X_{H2\ in} = Q_{gas\ r}X_{H2\ r} + Q_{H2\ p} \quad \left[\text{mol s}^{-1}\right] , \tag{4}$$

and by combining Eqs. (3) and (4):

$$Q_{H2\ p} = Q_{gas\ in}\frac{X_{H2\ in} - X_{H2\ r}}{1 - X_{H2\ r}} \quad \left[\text{mol s}^{-1}\right] . \tag{5}$$

Therefore, the hydrogen permeation molar rate $Q_{H2\ p}$ can be obtained from the total feed gas flow rate and the hydrogen feed/retentate concentration measurements by means of Eq. (5). The inlet gas flow rate $Q_{gas\ in}$ is measured by the FTC (Brooks SLA5850S), with an accuracy of 0.9%, with a confidence interval at 95%, giving a related standard uncertainty of 0.45%. The hydrogen inlet concentration $X_{H2\ in}$ is equal to the feed bottle concentration: its value of 2.926% mol ± 0.059% mol is given by calibration certificate with 95% confidence interval and related standard uncertainty of 1%. The hydrogen concentration in the retentate gas $X_{H2\ r}$ is measured during permeation tests by the gas chromatograph (μGC–SRA 3000), with a relative standard uncertainty of around 1% of measured value, estimated by means of a proper calibration procedure. A summary of the main variables and their relative (expressed in percentage) standard uncertainty is reported in Table I.

The standard uncertainty of $Q_{H2\ p}$ is then calculated as the combined uncertainty of the elements composing Eq. (5), according to GUM guidelines.[11] The absolute standard uncertainty in terms of molar flow is ±4.9 mol/s. Since $Q_{gas\ in}$ and $X_{\text{H2}\ in}$ are fixed during the test (see Sec. III.C), the relative standard uncertainty of $Q_{H2\ p}$ is mainly sensitive to the difference $X_{H2\ in} - X_{H2\ r}$. This results in a higher uncertainty for the lower differences (i.e., the lower $Q_{H2\ p}$ values), corresponding to a relative uncertainty varying from 5% to 12% over the measurements range of our tests.

III.B. Sodium Measurements

Hydrogen meters based on the nickel permeation membrane have been widely used for hydrogen detection in sodium reactors.[9,12] The hydrogen molar rate $(Q_{H2,DH})$ permeating from liquid sodium, which circulates inside the hydrogen meter membrane to vacuum to outside the membrane, can be expressed by combining Eqs. (1) and (2):

$$Q_{H2,DH} = \left(\frac{A}{\delta}\right)_{DH} pe_0 exp^{\frac{-E_p}{RT}}\left(\frac{y_{H,Na}}{K_{S,Na}} - \sqrt{P_{H2,vacuum}}\right) \left[\text{mol s}^{-1}\right] , \tag{6}$$

where $P_{H2,vacuum}$ is the hydrogen partial pressure on vacuum side and $y_{H,Na}$ varies in the range of 50 to 500 ppb, while

TABLE I

Standard Uncertainty of Measured and Constant Variables of the System according to GUM*

Variable	Unit	Instrument	Relative Standard Uncertainty
$T_{1,2,3}$	°C	Thermocouple K	0.4%
P_{gas}	bar a	Keller PT 23SY	0.25%
$Q_{gas\ in}$	mol s $^{-1}$	Brooks SLA5850S	0.45%
$X_{H2\ r}$	% mol	μGC- SRA 3000	1%
$X_{H2\ in}$	% mol	Air Liquide certificate	1%

*Reference 11.

$K_{S,Na}$ depends on temperature and its expression is given by Vissers[8]:

$$log(K_{S,Na}) = 0.86 - \frac{122}{T[K]} \quad [\text{ppm Torr}^{-0.5}] \ . \tag{7}$$

For this study, $K_{S,Na}$ is converted to (ppb $Pa^{-0.5}$). As a result, the ratio $\frac{y_{H,Na}}{K_{S,Na}}$ is orders of magnitude higher than the vacuum pressure so that the term in the brackets $\sqrt{P_{H2,vacuum}}$ can be neglected and Eq. (6) can be rewritten as

$$y_{H,Na} = \frac{Q_{H2,DH} K_{S,Na}}{\left(\frac{A}{\delta}\right)_{DH} pe_0 exp^{\frac{-E_p}{RT}}} \quad [\text{ppb}] \ . \tag{8}$$

By considering that the hydrogen molar flow rate $Q_{H2,DH}$ is proportional to the QMS signal corresponding to the molecular hydrogen peak, we get

$$y_{H,Na} = \frac{K_{MS} S_{MS,H2} K_{S,Na}}{\left(\frac{A}{\delta}\right)_{DH} pe_0 exp^{\frac{-E_p}{RT}}} \quad [\text{ppb}] \ , \tag{9}$$

where $S_{MS,H2}$ (Torr) is the mass spectrometer signal corresponding to mass 2 (i.e., molecular hydrogen) and K_{MS} (mol s^{-1} $Torr^{-1}$) is the calibration constant obtained by calibrated leak measurement. Therefore, by means of Eq. (9), it is possible to obtain an estimation of hydrogen molar concentration in liquid sodium.

III.C. Test Procedure and Test Conditions

When sodium is at a stable temperature and at low hydrogen content (typically $y_{H,Na}$ < 100 ppb), the CT section is isolated, so that purification stops and a stable hydrogen concentration is set up. Sodium circulates into the main circuit with a total flow rate of 2.5 m^3/h composed of 1 m^3/h through the TS and the remaining 1.5 m^3/h through the HT. A permeation test starts when the Ar-H_2 gas mixture is sent to the permeator at given pressure and flow rate, then hydrogen permeation takes place and measurements both in the gas and sodium sides are performed; these conditions are maintained stable for the entire test duration of 1 h. Then, permeation is stopped by sending pure argon into the permeator, thus purging the (tubular) membrane feed side from the residual hydrogen. As a new equilibrium concentration is obtained inside sodium, the following test can be launched with the same procedure. When the maximum allowed hydrogen concentration inside sodium of 500 ppb is approached, a purification session is performed by connecting the CT section to the main circuit.

Four temperatures were tested: T4 (375°C), T5 (400°C), T6 (425°C), and T7 (450°C); for each temperature, six gas total pressures were tested (2×10^5, 3.5×10^5, 5×10^5, 7×10^5, 9×10^5, and 10×10^5 Pa), at a fixed inlet gas flow rate of 200 Nml/min and at fixed inlet hydrogen concentration of 2.926% molar. The corresponding values of the inlet hydrogen partial pressure $P_{H2,gas}$ in the gas phase varies from 6×10^3 to 3×10^4 Pa.

IV. GAS-TO-SODIUM PERMEATION RESULTS

IV.A. Gas-Side Measurements

For each tested condition, $Q_{H2,p}$ has been calculated by means of Eq. (5). Theoretically, if we integrate Eq. (1) along the membrane considering a gas plug flow, $Q_{H2,p}$ should depend on gas pressure and temperature according to the following law:

$$Q_{H2,p} = \frac{A}{\delta} pe_0 e^{-\frac{Epe}{RT}} \left(\sqrt{\overline{P_{H2,gas}}} - \frac{y_{H,Na}}{K_{S,Na}} \right) \quad [\text{mol s}^{-1}] \ , \tag{10}$$

where $\overline{P_{H2,gas}}$ is the hydrogen mean partial pressure in the gas side calculated as the arithmetical mean between feed and retentate side, as follows:

$$\overline{P_{H2,gas}} = P_{gas} \left(\frac{X_{H2,in} + X_{H2,r}}{2} \right) [\text{Pa}] \ . \tag{11}$$

If we take P_{gas} as the measured gas pressure inside the permeator, $X_{H2,in}$ and $X_{H2,r}$ from the μGC measurements, for our experimental conditions $\sqrt{\overline{P_{H2,gas}}}$ vary from 74 to 166 $Pa^{0.5}$. These are 100 to 500 times greater than the ratio $\frac{y_{H,Na}}{K_{S,Na}}$, which can be neglected, so that Eq. (10) reduces to

$$Q_{H2,p} = \frac{A}{\delta} pe_0 e^{-\frac{Epe}{RT}} \sqrt{\overline{P_{H2,gas}}} \quad [\text{mol s}^{-1}] \ . \tag{12}$$

By plotting the $Q_{H2,p}$ measurements against $\sqrt{\overline{P_{H2,gas}}}$ for all experimental conditions tested, we can verify if the experimental results follow the integrated form of Richardson's law reported by Eq. (12). The results are reported in Fig. 3, plotted with their standard uncertainty bars; the absolute standard uncertainty in terms of molar

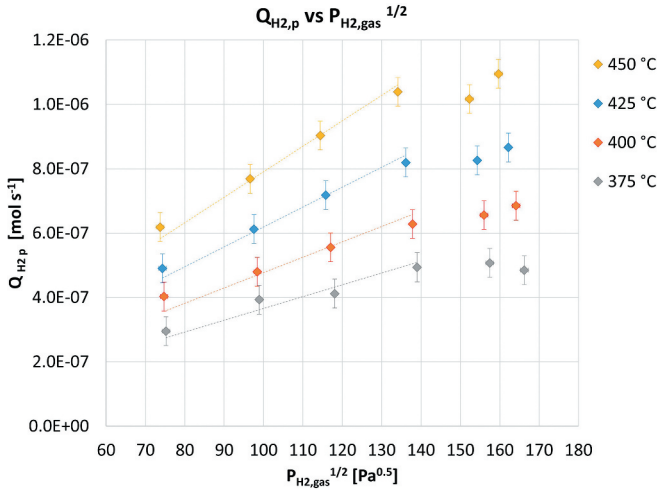

Fig. 3. Experimental hydrogen permeation rates from gas-side measurements.

flow is ±4.9 mol/s, corresponding to a relative uncertainty varying from 5% to 12% over the measurement range.

At each temperature, permeation increases linearly for the four lower pressures up to 140 Pa$^{0.5}$ (which corresponds to $\overline{P_{H2,gas}} = 2 \times 10^4$ Pa); this is highlighted by the linear regression dotted lines calculated imposing a y-intercept equal to zero in order to have a direct comparison with Eq. (12). Then, a clear discontinuity appears above 140 Pa$^{0.5}$, where the linear increment of permeation flux is no more respected and a pseudo-saturation condition seems to be achieved. In particular, the permeation decrease at 375°C–10 bar deviates from the theoretical fundamentals of permeation; these systematic deviations cannot been explained by the measurement uncertainty and let us suppose that permeation could be limited at higher pressures by other resistance mechanisms not considered by Eq. (12). A detailed discussion on this item is reported in Sec. IV.C.

Nevertheless, focusing on the "linear region," i.e., $\sqrt{P_{H2,gas}}$, from 70 to 140 Pa$^{0.5}$, an estimation of the permeability coefficient law can be obtained. In fact, by isolating the permeability coefficient in Eq. (12) and by applying a logarithm to both sides, one obtains the following equation:

$$ln\frac{Q_{H2,p}}{\frac{A}{\delta}\sqrt{P_{H2,gas}}} = -\frac{E_{pe}}{R}\frac{1}{T} + ln(pe_0) \quad . \tag{13}$$

For a given temperature, a mean value of the ratio $\frac{Q_{H2,p}}{\frac{A}{\delta}\sqrt{P_{H2,gas}}}$ (mol m^{-1} s^{-1} Pa$^{-0,5}$) is calculated by interpolation: Each value of this ratio represents the value of the permeability coefficient at the corresponding temperature. The logarithm of each ratio is then plotted as a function of 1/T [1/K], as shown in Fig. 4; the perfect linear dependence between the two, showed by the correlation coefficient R^2 equal to 0.9996, confirms the theoretical exponential dependence of permeability with temperature. Moreover, the interpolating line $y = -4902.3 \times -16.853$, compared to Eq. (13) where y is $\frac{Q_{H2,p}}{\frac{A}{\delta}\sqrt{P_{H2,gas}}}$ and x is $\frac{1}{T}$, gives $E_{pe} = 40757$ (J mol^{-1}) and $pe_0 = 4.8010^{-8}$ (mol m^{-1} s^{-1} Pa$^{-0.5}$). This result gives a permeability coefficient comparable to previous results provided by Sakamoto's review[13] for nickel, obtained by the authors at laboratory scale on small membranes in well controlled and homogeneous conditions. A permeability coefficient has been obtained for the same prototype, tested in a gas-vacuum configuration, in a previous work.[3] The results for the gas-sodium configuration obtained in this work are generally in accordance with them, even though a lower activation energy and higher permeability are found here. The slight deviation between these results and literature could be attributed to the pilot-scale effect, combined with the additional resistance mechanisms discussed in Sec. IV.C not considered by Eq. (12).

IV.B. Sodium-Side Measurements

As a permeation test begins, the hydrogen meter, which is located just after the permeator, detects an increment of $y_{H,Na}$. Since sodium is continuously circulating in a closed loop without purification, as long as the permeation goes on, $y_{H,Na}$ increases; once permeation is stopped, sodium reaches an equilibrium value of $y_{H,Na}$,

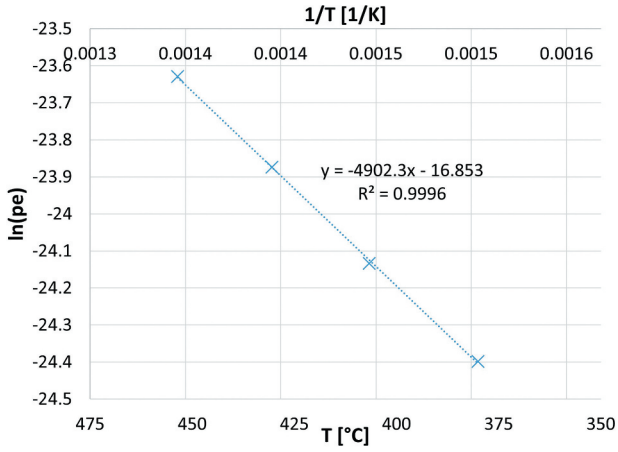

Fig. 4. Experimental mean permeability coefficients by linear regression.

proving that the permeated hydrogen has been homogeneously dissolved in the sodium loop. This dynamic is shown by the QMS signal, directly proportional to the hydrogen flow rate coming from the hydrogen meter, as reported in Fig. 5; it reports three consecutive permeation tests performed at 400°C at $\overline{P_{H2,gas}}$ of 5×10^3, 14×10^3, and 19×10^3 Pa, respectively. For each permeation test, the hydrogen signal is stable at initial and at final equilibrium, while it linearly increases over the test period due to the hydrogen enrichment of sodium that takes place.

Assuming that the hydrogen permeation flow is constant, an estimation of $Q_{H2,p}$ (mol_{H2}/s) can be obtained as follows:

$$Q_{H2,p} = \rho_{Na} V_{Na} \frac{y_{H,Na}(t_{eq}) - y_{H,Na}(t_0)}{2 t_p MM_H} 10^6 \left[\text{mol}_{\text{H2}}\ \text{s}^{-1}\right] , \quad (14)$$

where

ppb = concentration at the initial time and $y_{H,Na}(t_{eq})$ (ppb) at the equilibrium [calculated by means of Eq. (9)]

t_p = permeation time during the linear increase (s)

V_{Na} = sodium volume circulating in the closed circuit during permeation test (m^3)

ρ_{Na} = sodium density (kg m^3)

MM_H = hydrogen molar mass (g mol).

The factor 2 is applied to convert H moles to H_2 moles and the factor 10^6 to convert ppb to g/kg. A comparison between gas-side measurements by gas chromatography (μGC) and sodium-side measurements by mass spectrometer (QMS) is provided in Fig. 6; it reports $Q_{H2,p}$ measured with the two techniques at 375°C, 400°C, 425°C, and 450°C. A very good agreement is found at the two highest temperatures, with a percentage difference between the two measurement techniques below 15%; while at lower temperatures, where the detected hydrogen permeation rate is lower, deviations up to 40% are found. However, the mass spectrometer measurements should be considered as far less reliable since they are affected by quite a high uncertainty, coming from the spectrometer calibration procedure combined with the uncertainty of parameters composing Eq. (9) ($K_{S,Na}$ and permeability coefficients) and the uncertainty of the sodium volume in the loop. Ultimately, sodium-side measurements can be useful to validate the hydrogen mass balance through the permeator, but should not be used to obtain an accurate estimation of the hydrogen permeation rate. The role of the results shown in Fig. 6 is then to confirm that the hydrogen content variation of sodium corresponds effectively to the hydrogen source coming from the permeator, at least an order of magnitude. This result could be trivial, but it demonstrates a reliable validation of the entire process application and measurement techniques and very promising perspectives for a precise control of dissolved hydrogen concentration in sodium circuits.

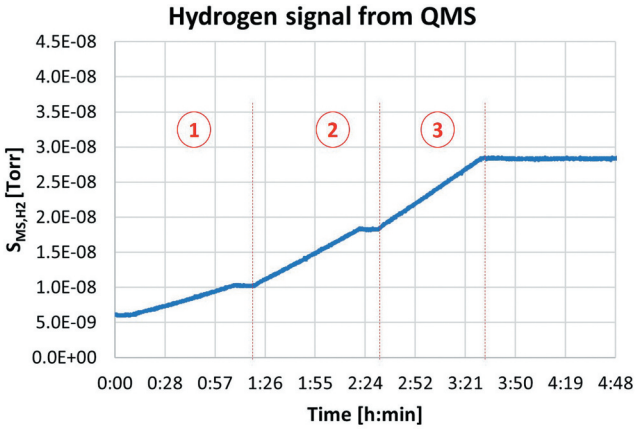

Fig. 5. Hydrogen signal from QMS: evolution during permeation tests at 400°C and (1) 5×10^3 Pa, (2) 14×10^3 Pa, and (3) 19×10^3 Pa.

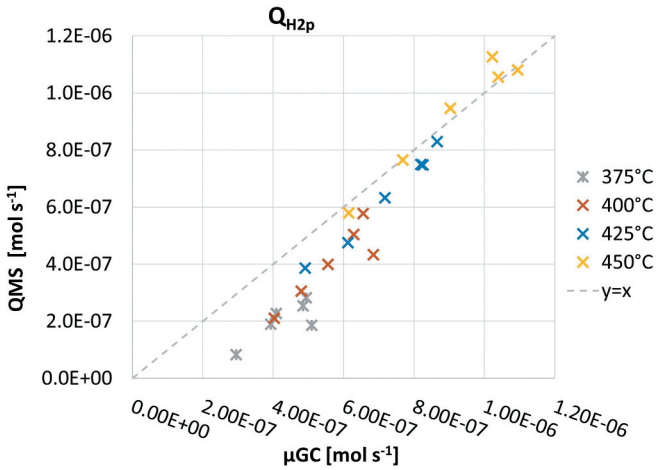

Fig. 6. Experimental hydrogen permeation rates at 375°C, 400°C, 425°C, and 450°C: comparison between gas (μGC) and sodium (QMS)–side measurements.

IV.C. Discussion on Deviations at $\overline{P_{H2,gas}} > 2 \times 10^4$ Pa

As pointed out in Sec. IV.A, deviations from the linearity between $Q_{H2,p}$ and $\sqrt{\overline{P_{H2,gas}}}$ have been observed above 140 $Pa^{0.5}$ (corresponding to $\overline{P_{H2,gas}} = 2 \times 10^4$ Pa), leading to an increase of $Q_{H2,p}$ lower than expected, or even to a decrease (see Fig. 3, point at 375°C–166 $Pa^{0.5}$). This means that in this range of pressures, the theoretical law in Eq. (12), based on the hypothesis of a diffusion-limited permeation, is no more representative of our experimental results. Therefore, it seems reasonable to think that some additional hydrogen transport or resistance mechanisms, not considered by the diffusion-limited permeation law, could take place when hydrogen pressure exceeds a given threshold value. However, such kinds of permeability deviations have never been observed in pure nickel samples of similar thickness for the same temperature and hydrogen pressure range.[13] In this sense, it is worth noting that our tests were performed with a diluted hydrogen gas mixture, and the hydrogen pressure increase has been obtained by simply increasing the total gas pressure from 2×10^5 to 10×10^5 Pa. This significant increase of the gas pressure during tests provides a consequent increase of the mechanical stress on the membrane, as well as changes in the gas-mixture properties and interactions with the membrane's feed surface. Taking into account this consideration, we propose four possible effects not considered by the diffusion-limited permeation model, which could eventually explain the observed deviation at high pressures:

1. *The saturation of the membrane's surface active sites, eventually occurring at high pressures, already observed by Waelbroek*[14]: However, the results of Waelbroek do not fit with our experimental range.

2. *The gas-phase polarization effect, which can limit permeation at certain conditions of high permeation rates and gas pressures*[15]: This effect has been observed for very thin Pd/Ag membranes,[16] where the permeation convective contribution is comparable to the gas convection. To a first approximation analysis, this does not seem to be our case.

3. *The competitive adsorption of argon at the membrane's feed surface, already observed for palladium membranes and gas mixtures containing CO, CO_2, or N_2 (Refs. 17 and 18)*: No evidence has been found for argon, but we cannot exclude that it could take place here.

4. *The hydrogen transport by dislocations induced by the high mechanical constraint*: If the membrane is affected by deformations, provided by the increasing mechanical stress, it is possible that dislocations are generated inside the nickel lattice and hydrogen pure diffusive transport is then affected,[19] thus deviating from the diffusion-limited permeation law.

In conclusion, the most probable phenomena taking place at the highest pressures seem to be the effects 3 and 4; nevertheless, these are only hypotheses and further studies will be needed to confirm them or not.

V. CONCLUSIONS

This work provides preliminary results for the control of the permeation transfer of hydrogen from a diluted gas phase into flowing liquid sodium, thanks to tests performed on a permeator prototype installed in a dedicated sodium loop reproducing operating conditions similar to an SFR's secondary circuits. Permeation was tested at temperatures from 375°C to 450°C and hydrogen partial pressures in the gas phase from 5×10^3 to 3×10^4 Pa. Measurements on the gas side provide estimation values of the permeation mass transfer rate $Q_{H2,p}$, with a relative standard uncertainty of the order of ±10%. Results show a good agreement with the theoretical diffusion-limited permeation law for hydrogen pressures below 2×10^4 Pa, while a deviation from the theory is found at higher pressures. By linear regression of experimental data in the linear range, the following permeability coefficients were obtained: $E_{pe} = 40757$ (J mol^{-1}) and $pe_0 = 4.80\ 10^{-8}$ (mol m^{-1} s^{-1} $Pa^{-0.5}$). Measurements on the sodium side, performed with a conventional hydrogen meter already used in SFRs, provide values of the hydrogen concentration inside sodium $y_{H,Na}$: These results, compared to the gas-side measurements, validate the global hydrogen mass balance. Finally, both the permeator prototype and the hydrogen meter installed on the experimental sodium loop give coherent results; the permeation rate varies with temperature and gas pressure according to an integrated form of Richardson's law, reported in Eq. (12), for hydrogen partial pressures lower than 2×10^4 Pa. This work constitutes a good basis for the validation of the permeator prototype for the purpose of a future application to SFRs for a precise control and adjustment of dissolved hydrogen concentration as an efficient solution for the management of tritium inventory and its release into the atmosphere.

APPENDIX

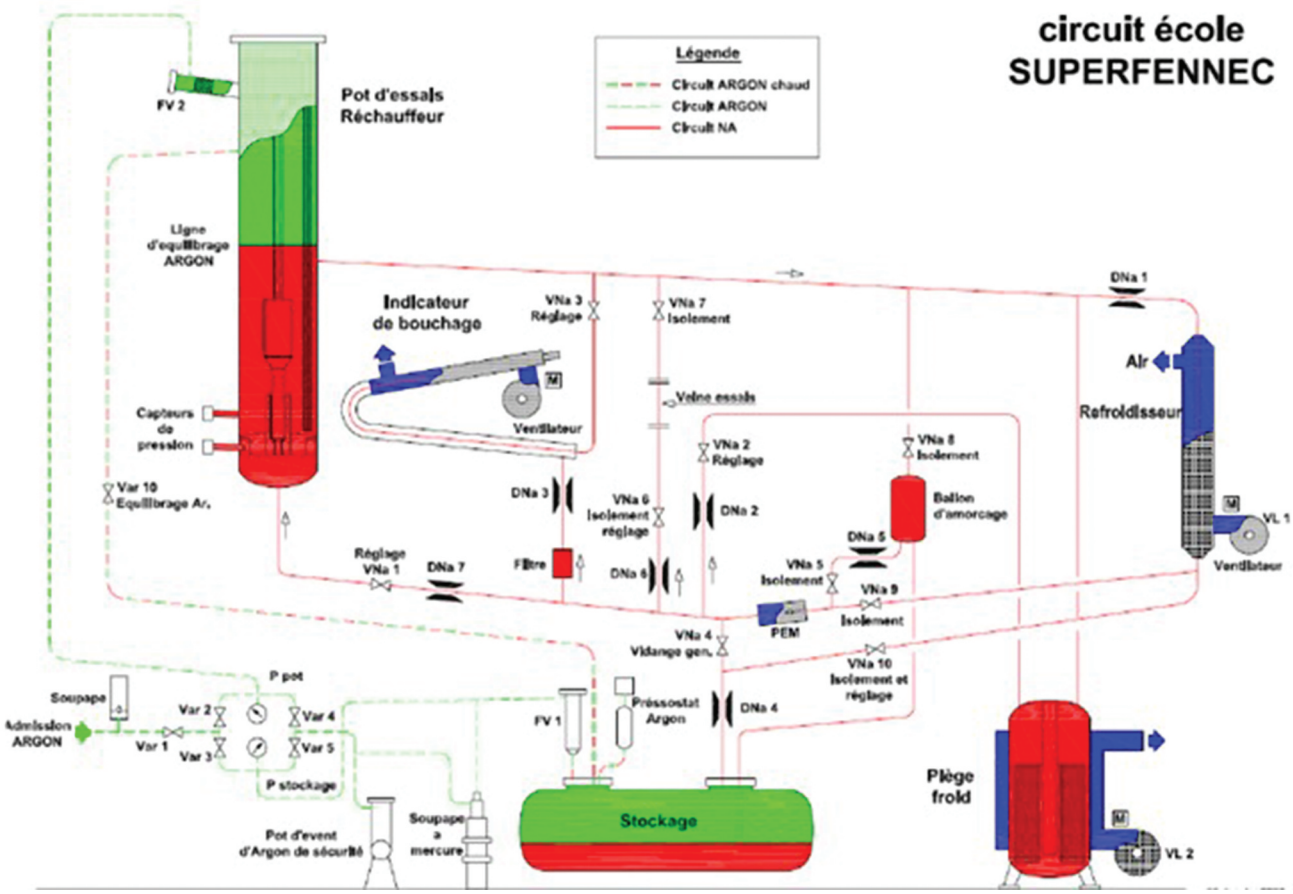

Fig. A.1. Detailed flowchart of the circuit.

Fig. A.2. Picture of the TS: sodium circuit (orange arrows), gas circuit (blue arrows), and vacuum line (green arrows).

Nomenclature

A = membrane surface (m^2)
C = molar concentration (mol m^{-3})
E_p = permeation activation energy (J mol^{-1})
K_{MS} = mass spectrometer constant (mol s^{-1} Torr $^{-1}$)
K_S = Sieverts constant (mol m^{-3} $Pa^{-0.5}$)
MM = molar mass (g mol^{-1})
P = pressure (Pa)
pe_0 = permeability: pre-exponential constant (mol m^{-1} s^{-1} $Pa^{-0.5}$)
Q = molar flow rate (mol s^{-1})
R = gas universal constant (J mol^{-1} K^{-1})
S_{MS} = mass spectrometer signal (Torr)
ρ = density (kg m^{-3})

T = temperature (°C)

t = time (s)

$\dot{V}$ = volumetric flow rate ($m^3\ s^{-1}$)

V = volume (m^3)

X = molar fraction (% mol)

y = mass fraction (ppb)

Greek

δ = membrane thickness (m)

Subscripts

gas = gas phase

Na = sodium phase

H_2 = molecular hydrogen

H = atomic hydrogen

in = permeator inlet side

r = permeator retentate side

p = permeator permeate side

f = permeator feed side

ORCID

Pietro Brazzale http://orcid.org/0000-0002-3347-9543

References

1. C. LATGE, "Sodium Quality Control; French Developments from Rapsodie to EFR," Kyoto (2009); http://inis.iaea.org/Search/search.aspx?orig_q=RN:41069931 (accessed Dec. 11, 2019).
2. L. CACHON et al., "Innovative Power Conversion System for the French SFR Prototype, ASTRID," American Nuclear Society,La Grange Park, Illinois (July 2012); https://www.osti.gov/biblio/22105979-innovative-power-conversion-system-french-sfr-prototype-astrid (accessed Dec. 11, 2019).
3. P. BRAZZALE et al., "Modelling of a Hydrogen Permeation Process from Gas Phase Towards Liquid Sodium and Experimental Set-up for Prototype Testing," *Chem. Eng. Res. Des.*, **159**, 555 (July 2020); https://doi.org/10.1016/j.cherd.2020.05.012.
4. O. W. RICHARDSON, J. NICOL, and T. PARNELL, "I. the Diffusion of Hydrogen Through Hot Platinum," *London, Edinburgh Dublin Philos. Mag. J. Sci.*, **8**, *43*, 1 (July 1904); https://doi.org/10.1080/14786440409463168.
5. T. GNANASEKARAN, "Thermochemistry of Binary Na-NaH and Ternary Na-O-H Systems and the Kinetics of Reaction of Hydrogen/Water with Liquid Sodium—A Review," *J. Nucl. Mater.*, **274**, *3*, 252 (Sep. 1999); https://doi.org/10.1016/S0022-3115(99)00072-0.
6. J.-P. MAUPRE, "Study of the Na-C-O and Na-H-O Ternary Systems in the Sodium Rich Corner," PhD Thesis, Université de Provence—Centre Saint Charles (1978).
7. A. C. WHITTINGHAM, "An Equilibrium and Kinetic Study of the Liquid Sodium-Hydrogen Reaction and Its Relevance to Sodium-Water Leak Detection in LMFBR Systems," *J. Nucl. Mater.*, **60**, *2*, 119 (May 1976); https://doi.org/10.1016/0022-3115(76)90157-4.
8. D. R. VISSERS et al., "A Hydrogen-Activity Meter for Liquid Sodium and Its Application to Hydrogen Solubility Measurements," *Nucl. Technol.*, **21**, *3*, 235 (Mar. 1974); https://doi.org/10.13182/NT74-A31394.
9. K. PAUMEL, "Comparative Tests of Two Hydrogen-Meter Technologies in the Phenix Reactor," presented at the NPIC&HMIT, San Diego, California, July 22–26, 2012.
10. S. K. LEE et al., "Study of an Experimental System for Hydrogen Permeation in Thin-Solid Materials for Fusion Plasma Research," *Curr. Appl Phys.*, **11**, *5*, S99 (Sep. 2011); https://doi.org/10.1016/j.cap.2011.05.005.
11. BUREAU INTERNATIONAL DES POIDS ET MESURES, "Guide to the Expression of Uncertainty in Measurement (GUM)," JCGM, 100, 2008 (2008).
12. D. R. VISSERS et al., "A Hydrogen Monitor for Detection of Leaks in LMFBR Steam Generators," *Nucl. Technol.*, **12**, *2*, 218 (Oct. 1971); https://doi.org/10.13182/NT71-A31029.
13. Y. SAKAMOTO, "Nickel-Hydrogen System," *Solid State Phenom.*, **73-75**, 137 (2000); https://doi.org/10.4028/www.scientific.net/SSP.73-75.137.
14. F. WAELBROECK et al., "Influence of Bulk and Surface Phenomena on the Hydrogen Permeation through Metals," Kernforschungsanlage Juelich G.m.b.H., Germany (JUEL–1966, 1984); http://inis.iaea.org/Search/search.aspx?orig_q=RN:16053332 (accessed June 6, 2019).
15. A. MOURGUES and J. SANCHEZ, "Theoretical Analysis of Concentration Polarization in Membrane Modules for Gas Separation with Feed Inside the Hollow-Fibers," *J. Membr. Sci.*, **252**, *1–2*, 133 (Apr. 2005); https://doi.org/10.1016/j.memsci.2004.11.024.
16. J. CATALANO, M. G. I. BASCHETTI, and G. C. SARTI, "Influence of the Gas Phase Resistance on Hydrogen Flux Through Thin Palladium-Silver Membranes," *J. Membr. Sci.*, **339**, *1–2*, 57 (Sep. 2009); https://doi.org/10.1016/j.memsci.2009.04.032.

17. F. GALLUCCI et al., "The Effect of Mixture Gas on Hydrogen Permeation Through a Palladium Membrane: Experimental Study and Theoretical Approach," *Int. J. Hydrogen Energy*, **32**, *12*, 1837 (Aug. 2007); https://doi.org/10.1016/j.ijhydene.2006.09.034.

18. W.-H. CHEN and J. ESCALANTE, "Influence of Vacuum Degree on Hydrogen Permeation Through a Pd Membrane in Different H_2/N_2 Gas Mixtures," *Renew. Energy*, **155**, 1245 (Aug. 2020); https://doi.org/10.1016/j.renene.2020.04.048.

19. A. OUDRISS, "Influence des hétérogénéités métallurgiques sur les processus de diffusion et de piégeage de l'hydrogène dans le nickel," PhD Thesis, Université de La Rochelle (2012).